Virchows Arch (2015) 466:161–168
DOI 10.1007/s00428-014-1696-1

ORIGINAL ARTICLE

Intestinal metaplasia of the sinonasal mucosa adjacent to intestinal-type adenocarcinoma. A morphologic, immunohistochemical, and molecular study

Alessandro Franchi · Annarita Palomba · Lucia Miligi · Valentina Ranucci · Duccio Rossi Degli Innocenti · Antonella Simoni · Monica Pepi · Marco Santucci

Received: 4 August 2014 / Revised: 5 November 2014 / Accepted: 17 November 2014 / Published online: 28 November 2014

Abstract It has been hypothesized that the development of sinonasal intestinal-type adenocarcinoma (ITAC) occurs through intestinal metaplasia (IM) of the respiratory and/or glandular epithelium. The aim of this study was to characterize the histological, immunohistochemical, and molecular features of sinonasal IM. Histologic slides from 29 consecutive surgical specimens of ITAC were retrieved. Sections were stained for CDX2, cytokeratin 20 (CK20), MUC2, and p53. The status of TP53 gene exons 4–9 was assessed separately in areas of IM and in ITAC. Foci of IM were detected in eight cases (27.5 %). They were all positive for CK20 and CDX2, while MUC2 was detected in six cases (75 %). In six cases (75 %), the metaplastic foci showed signs of dysplasia, including nuclear enlargement with increased nucleus to cytoplasm ratio, nuclear hyperchromasia, loss of nuclear polarity, and presence of prominent nucleoli. P53 nuclear immunoreactivity was observed in four cases. TP53 gene sequencing was successfully performed in six cases and revealed the same mutation in both IM and ITAC in two cases (c.832C>T and c.215G>C), while another ITAC showed a mutation that was not present in the adjacent IM (c.536A>G). In conclusion, our study suggests a possible clonal relationship between areas of sinonasal IM and ITAC, indicating that IM may represent a precursor lesion of ITAC. Improving the knowledge on the morphological and molecular features of IM is a key step to identify reliable biomarkers to determine the risk of sinonasal ITAC development.

Keywords Nasal cavities · Paranasal sinuses · Intestinal metaplasia · Intestinal-type adenocarcinoma · Immunohistochemistry · TP53 gene

A. Franchi (✉) · A. Simoni · M. Pepi · M. Santucci
Section of Anatomic Pathology, Department of Surgery and Translational Medicine, University of Florence, Largo Brambilla 3, 50134 Florence, Italy
e-mail: franchi@unifi.it

A. Palomba
Section of Histopathology, Department of Biomedicine, Azienda Ospedaliera Universitaria Careggi, Florence, Italy

L. Miligi
Unit of Environmental and Occupational Epidemiology, ISPO—Cancer Prevention and Research Institute, Florence, Italy

V. Ranucci
Department of Anatomic Pathology, Catholic University, Rome, Italy

D. R. D. Innocenti
Department of Clinical and Experimental Medicine, University of Florence, Florence, Italy

Introduction

Sinonasal intestinal-type adenocarcinoma (ITAC) is a rare tumor that develops preferentially in individuals exposed to wood dust and leather dust. It originates preferentially from the ethmoid, and it is characterized by a locally aggressive clinical course, with repeated local recurrences, while distant metastases are not frequent. Therefore, an early diagnosis is necessary in order to improve the prognosis. However, the carcinogenic process leading to the development of ITAC is poorly understood and no precursor lesion has been identified so far with certainty, although it seems reasonable to think that the development of ITAC may occur through intestinal metaplasia (IM) of the respiratory and/or glandular epithelium of the sinonasal mucosa. Indeed, areas of IM have been observed in the vicinity of invasive ITAC and they have been considered as putative preneoplastic lesions [1–3].

The IM is part of the carcinogenic sequence that leads to the development of gastric adenocarcinoma of the intestinal-type and esophageal carcinoma in Barrett's esophagus. In

these settings, the morphological and molecular bases of the metaplastic process have been widely investigated. Moreover, the presence of IM with nuclear atypia has been related to a high risk of developing an adenocarcinoma [4]. On the other hand, the immunophenotypic and molecular features of sinonasal IM are largely unknown. In this study, we performed a systematic review of a series of surgically treated ITAC in search of areas of IM of respiratory and glandular epithelium of the sinonasal mucosa. To this aim, we reviewed hematoxylin and eosin stained slides and performed an immunohistochemical analysis with markers of intestinal differentiation. Moreover, we performed an analysis of the status of TP53 gene of metaplastic areas and corresponding adenocarcinomas.

Patients and methods

Case selection

In the period 1995–2010, forty-two cases of ITAC were histologically diagnosed at our department. In twenty-nine of these (69 %), material obtained from surgical resection specimens was available. All the hematoxylin and eosin stained glass slides were retrieved from our files and carefully re-examined for the histological appearance of the non-neoplastic surface epithelium and glands adjacent to the tumor.

The type of epithelial covering (respiratory type only; areas of squamous metaplasia; areas of intestinal metaplasia) was evaluated in each case, together with the presence of dysplastic changes. These were defined, in analogy with gastric dysplasia [4], as the presence of nuclear hyperchromasia and enlargement, loss of nuclear polarity, and presence of nucleoli.

Fragments of inflamed sinonasal mucosa (n=4) and inflammatory polyps (n=6) were used as controls for the immunohistochemical staining.

Immunohistochemistry

In order to confirm the intestinal phenotype in areas of metaplastic epithelium, we performed an immunohistochemical staining on serial sections for markers indicative of an intestinal phenotype, including CDX2, cytokeratin 20 (CK20), and MUC2. These markers are also expressed by sinonasal ITAC but not by sinonasal respiratory epithelium and normal seromucous glands [2, 5]. In addition, we examined the expression of p53 and cyclin D1 oncoproteins, both in non-neoplastic epithelium and ITACs, as well as the Ki67 labeling index (Ki67LI), expressed as percentage of positive cells in the area with the highest density of cells staining positively. The Ki67LI was assessed separately in normal epithelia, in areas of IM and in adenocarcinoma tissue, counting at least 200 cells in each case.

For immunohistochemical staining, paraffin section (5 μm thickness) were dewaxed, hydrated, and immunostained after inactivation of endogenous peroxidase using the BenchMark® XT (Ventana, Tucson, AZ) stainer and revealed with the iVIEW DAB detection kit, yielding a brown reaction product. Table 1 reports the antibody source, dilution, and antigen retrieval protocols used. After the staining run was complete, the slides were removed from autostainer, counterstained with hematoxylin, dehydrated, and mounted with permanent mounting medium. As negative controls, we substituted the primary antibody with a Ventana dispenser filled with non-immune serum at the same concentration for each immunohistochemical reaction.

An immunostaining was considered positive when >10 % of cells expressed the marker.

TP53 gene sequencing

Hematoxylin and eosin stained slides, as well as immunohistochemical slides stained with markers of intestinal differentiation, were first carefully examined in order to select areas of IM that were clearly separated from tumor areas. Ten serial sections (5 μm thickness) were obtained from one paraffin-embedded tissue block. Tissue fragments were microdissected using stereomicroscopic visualization from blank, deparaffinized slides, in order to separate the metaplastic epithelium and the areas of the tumor. The DNA was purified with QIAamp® DNA FFPE Tissue Kit (Qiagen, Hilden, DE) according to the manufacturer's protocol, and the DNA concentration was assessed spectrophotometrically using NanoDrop 2000 (Thermo Scientific).

Table 1 Antibody source, dilution, and antigen retrieval protocols used

Antibody	Clone and source	Species and titration	Antigen retrieval
CDX2	EPR2764Y, Ventana, Tucson, AZ	Rabbit, prediluted	CC1, 60 min
CK20	SP33, Ventana	Rabbit, prediluted	CC1, 60 min
MUC2	MRQ18, Ventana	Mouse, prediluted	CC1, 60 min
p53	DO7, Ventana,	Mouse, prediluted	CC1, 60 min
Cyclin D1	SP4R, Ventana	Rabbit, prediluted	CC1, 60 min
Ki67	30-9, Ventana	Mouse, prediluted	CC1, 60 min

Table 2 Primers and annealing temperature employed in the analysis of the TP53 gene

	Primers	Annealing T
Exon 4 forward	GCTCTTTTCACCCATCTACA	53 °C
Exon 4 reverse	ACCGTGCAAGTCACAGACTT	
Exon 5 forward	CTCTTCCTACAGTACTCCCCTGCC	62 °C
Exon 5 reverse	GCCCCAGCTGCTCACCATCGCTA	
Exon 6 forward	GATTGCTCTTAGGTCTGGCCCCT	62 °C
Exon 6 reverse	GGCCACTGACAACCACCCTTAAC	
Exon 7 forward	GTGGTTATCTCCTAGGTTGGCTCT	62 °C
Exon 7 reverse	CAAGTGGCTCCTGACCTGGAGTC	
Exon 8 forward	AGTAGTGGTAATCTACTGGGACGG	54 °C
Exon 8 reverse	GCAGCTCGTGGTGAGGCT	
Exon 9 forward	CCCTTCAGGTACTAAGTCTTGG	55 °C
Exon 9 reverse	CGAAATGCCCCAATTGCAGG	

PCR reaction for TP53 gene exons 4, 5, 6, 7, 8, and 9 was performed using the primers shown in Table 2. The reaction was carried out in a volume of 50 μl, with 1.5 mM $MgCl_2$, 10 pmol of each primer, and 2 U PerfectTaq Plus DNA Polymerase (5-PRIME) with 100 ng of DNA template. The cycle conditions were 60 s at 95 °C, 60 s at specific annealing temperature (Table 2), and 60 s at 72 °C for 32 cycles. A 10-min final extension was added. The amplification was performed in a 2720 Thermal Cycler (Applied Biosystems, USA). The amplification products were purified with HiYield™ Gel/PCR DNA Fragments Extraction kit (RBC Bioscience) according to the manufacturer's protocol.

Subsequently, we performed cycle sequencing reaction of purified PCR products using the TP53 forward primers and BigDye® Terminator v1.1 Cycle Sequencing Kit (Applied Biosystems, USA) according to the manufacturer's protocol. The sequencing products were purified using ZR DNA Sequencing Clean-up Kit™ (Zymo Research USA).

The samples were analyzed using the AbiPrism 310 Genetic Analyzer (Applied Biosystems, USA). The sequence results for each sample were analyzed using SeqScape® Software v2.5 (Applied Biosystems, USA) to verify the sequencing results and identify the possible mutations.

Statistical analysis

All statistical tests were performed using SPSS software (release 17.0). Mann–Whitney and Kruskal–Wallis tests were used to compare the Ki67 labeling index between normal epithelia, metaplastic epithelia, and ITAC. All tests were conducted as two-tail tests, with *P* values less than or equal to .05 considered statistically significant.

Results

Histopathology and immunohistochemistry

Table 3 summarizes the clinical, histological, immunohistochemical, and molecular features of the cases of sinonasal IM and ITAC that form the object of this study. Foci of IM were detected in eight cases (27.5 %) and were better recognized with the use of immunohistochemical markers. They were all positive for CK20 and CDX2, while MUC2 was detected in six cases (75 %). They presented as groups of cells separated by areas of normal respiratory epithelium, which localized mainly in the basal layers, whereas the superficial layers often consisted of ciliated respiratory cells (Fig. 1). In one case, mucous cells which were positive for CK20, CDX2, and

Table 3 Summary of the clinical, histological, immunohistochemical, and molecular features of eight cases of sinonasal intestinal metaplasia adjacent to sinonasal intestinal-type adenocarcinoma

Patient	Gender/age	Occupational exposure	Site of IM	Dysplasia	CK20		CDX2		MUC2		p53		Cyclin D1		TP53	
					IM	C	IM	C	IM	C	IM	C	IM	C	IM	C
1	M/64	Woodworker	Superficial	Yes	+	+	+	+	+	+	+	+	+	+	ND	ND
2	M/52	Woodworker	Superficial	No	+	+	+	+	−	−	−	−	−	−	WT	WT
3	M/62	Unknown	Superficial	Yes	+	+	+	+	+	+	−	−	+	+	ND	ND
4	M/81	Leatherworker	Superficial and glandular	Yes	+	+	+	+	+	+	−	−	+	+	WT	WT
5	M/57	Woodworker	Superficial	Yes	+	+	+	+	−	−	+	+	+	+	Exon 8 P278S	Exon 8 P278S
6	M/68	Leatherworker	Superficial	Yes	+	+	+	+	+	+	+	+	+	+	WT	Exon 5 H179R
7	M/66	Leatherworker	Superficial and glandular	Yes	+	+	+	+	+	+	+	+	+	+	WT	WT
8	M/59	Woodworker	Superficial and glandular	No	+	+	+	+	+	+	+	+	+	+	Exon 4 R72P	Exon 4 R72P

IM intestinal metaplasia, *C* Carcinoma, *CK* cytokeratin, *ND* not done

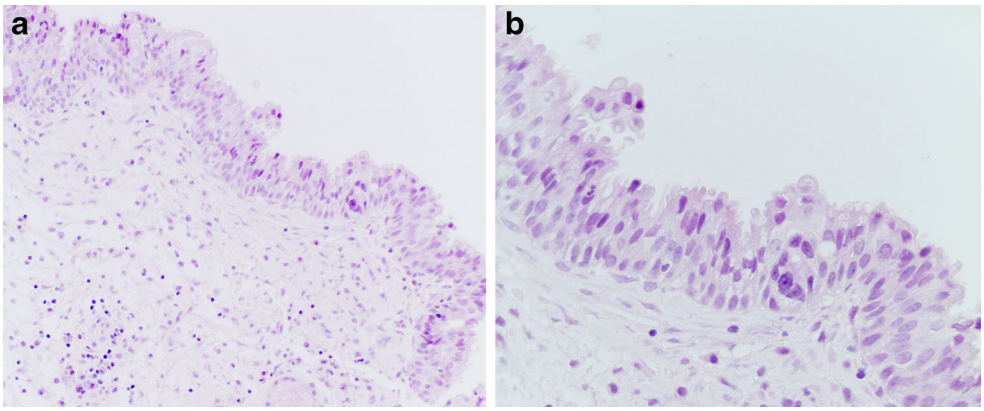

Fig. 1 **a** and **b** Areas of intestinal metaplasia of the surface sinonasal epithelium adjacent to intestinal-type adenocarcinoma. Single elements and groups of metaplastic cells, interspersed within the epithelium, showing hyperchromatic enlarged nuclei, sometimes with large nucleoli. Areas like this were considered dysplastic

MUC2 were associated with the areas of IM (Fig. 2). In three cases, metaplastic foci positive CK20, CDX2, and MUC2 were also observed in the seromucous glands of the lamina propria (Fig. 3). These consisted of small groups of cells interspersed within the ducts and acini, which in turn were negative for all the immunohistochemical markers. Scattered cells of the basal layers of surface epithelium and of the mucosal glands showed nuclear positivity for cyclin D1, including metaplastic areas positive for CK20 and CDX2 (Fig. 4). All ITACs showed intense and diffuse nuclear positivity for cyclin D1.

Metaplastic cells within surface epithelium had a cylindrical or cubical shape, eosinophilic cytoplasm and round to oval nucleus. Goblet cells were identified in one of the specimens. In six cases (75 %), the metaplastic foci were partially associated with dysplastic changes, consisting of nuclear enlargement, with increased nucleus to cytoplasm ratio, nuclear hyperchromasia, loss of nuclear polarity, and presence of prominent nucleoli (Fig. 1).

No significant difference was observed in terms of proliferative activity evaluated as Ki67LI between the metaplastic foci and normal epithelia (5.93±3.44 SD versus 4.75±1.79 SD, P=0.64), while a significant increase was observed for ITACs, which showed a Ki67LI of 33.95±21.82 SD (P<0.001).

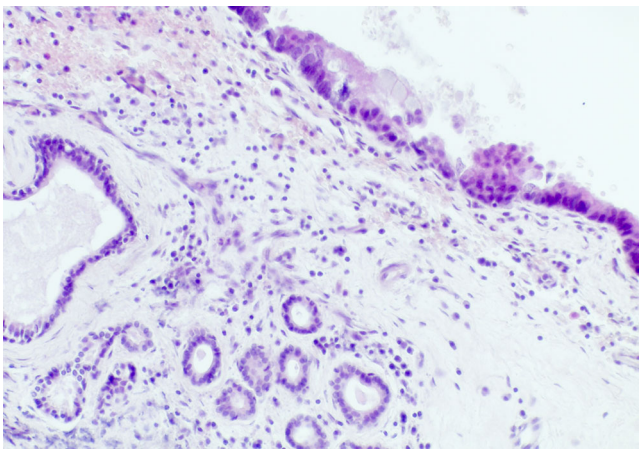

Fig. 2 Area of intestinal metaplasia of the surface epithelium with presence of superficial mucous producing cells

Areas of squamous metaplasia of the surface epithelium were identified in four cases (13.7 %), one of which showed also foci of IM. The squamous metaplastic epithelium was negative for CK20, CDX2, and MUC2.

Fragments of inflamed sinonasal mucosa and inflammatory polyps were used as controls and CK20, CDX2, and MUC2 were negative in the surface and glandular epithelia. Nuclear immunoreactivity for cyclin D1 was detected mainly in the basal layers of surface epithelia and in scattered cells in the glands of the lamina propria (data not shown).

TP53 analysis

P53 nuclear immunoreactivity was observed in foci of IM in five of the cases, including surface and glandular epithelium, while normal epithelial cells without signs of IM were always negative (Fig. 2). The corresponding adenocarcinomas were positive to a similar degree.

TP53 gene sequencing of the microdissected areas of IM and ITAC was performed on exons 4, 5, 6, 7, 8, and 9 in five cases. Two cases were not analyzed at the molecular level, because the areas of IM were judged to be too small and sparsely distributed. The results are summarized in Table 3. Two cases presented the same mutation in the IM and in the adenocarcinoma, which consisted of point mutation in exon 8 (c.832C>T) and a point mutation in exon 4 (c.215G>C). In a further case, we detected a mutation in exon 5 (c.536A>G), which was present only in the adenocarcinoma tissue, but not in the IM areas (Fig. 5).

Discussion

Improving the knowledge on the morphological and molecular features of IM in the sinonasal mucosa appears to be a key step to identify reliable biomarkers to determine the risk of sinonasal ITAC development. Despite several studies have

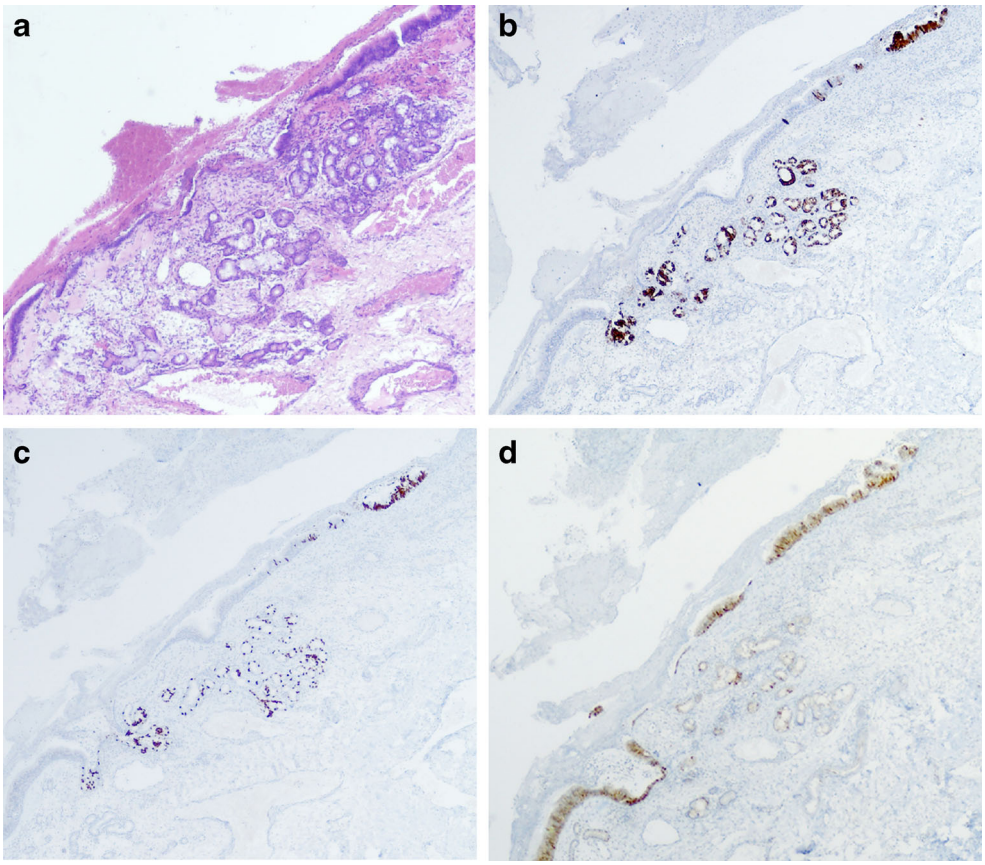

Fig. 3 Foci of intestinal metaplasia of the surface and glandular epithelia of the nasal mucosa. Serial sections. **a** Hematoxylin and eosin. **b** Cytokeratin 20 immunostaining. **c** CDX2 immunostaining. **d** Cyclin D1 immunostaining

contributed to define the molecular and phenotypic changes associated with ITAC [6], the critical events that contribute to the initiation and progression of this tumor are still to be elucidated. One of the major problems is that precursor lesions of ITAC are not well defined. However, a key event in the development of ITAC is likely to be the transdifferentiation of the sinonasal surface respiratory and/or glandular epithelium to an intestinal phenotype. In their study of seven cases of

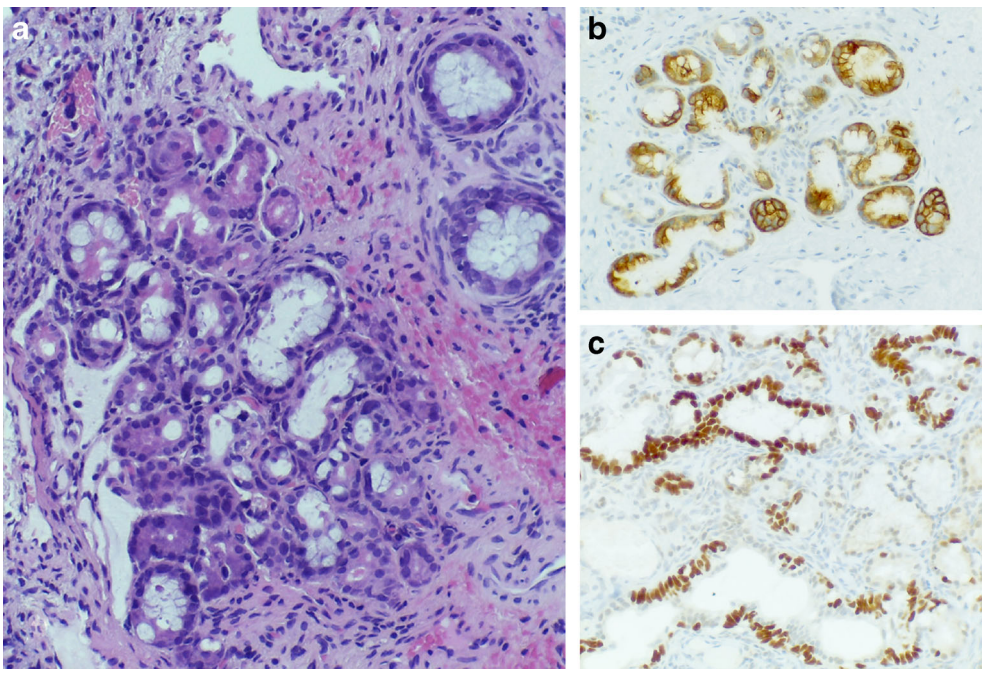

Fig. 4 Intestinal metaplasia of the seromucous glands of the sinonasal mucosa. **a** Hematoxylin and eosin showing interspersed cells with enlarged hyperchromatic nuclei. **b** Positive immunostaining for cytokeratin 20. **c** Positive immunostaining for CDX2

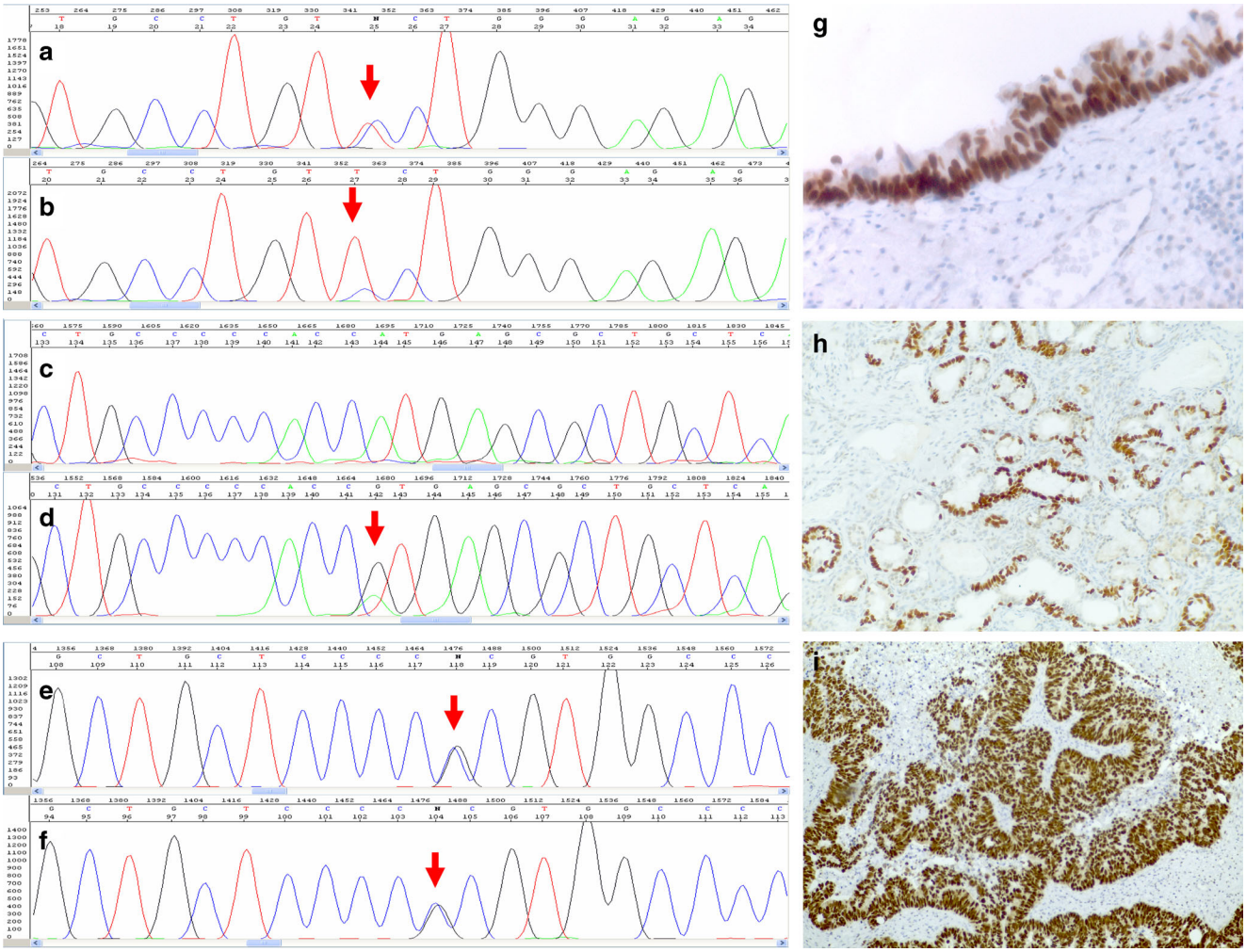

Fig. 5 The left panels illustrate TP53 gene mutations (indicated by *arrow*) in sinonasal intestinal metaplasia (IM) and intestinal-type adenocarcinoma (ITAC). All identified mutations are single-nucleotide polymorphism (SNP). **a** and **b** The same exon 8 P287S mutation is present both in IM (**a**) and ITAC (**b**). **c** and **d**. An exon 5 H179R mutation is present in the ITAC (**d**) but not in the IM (**c**). **e** and **f**. AN exon 4 R72P mutation is detected both in IM (**e**) and ITAC (**f**). Coexistence of wild-type and mutant sequence in the mutant sample represents a heterozygous mutation. The right panels illustrate p53 immunohistochemical staining of the same case of panels **a** and **b** on the left. Diffuse and intense nuclear immunohistochemical staining for p53 is detected in areas of IM of the surface epithelium (**g**) and of the mucosal glands (**h**), as well as in the adjacent ITAC (**i**)

ITAC, Choi and coworkers observed that in four instances, the sinonasal mucosa overlying the tumor exhibited microscopic areas of intestinal metaplasia interspersed within the respiratory-type epithelium, which were positive for CK20 and negative for CK7 [1]. Similarly, Kennedy et al. [2] reported one case of ITAC with an adjacent focus of intestinal metaplasia, which showed an immunophenotype CK7-/CK20+/CDX2+/villin+ similar to the invasive carcinoma, whereas the non-neoplastic mucosa retained its CK7+/CK20-/CDX2-/villin- phenotype. More recently, Vivanco et al. identified areas of CK20 positive IM in 8 % of samples of tumor-adjacent mucosa from ITAC patients [3], which involved both surface epithelia and glands. Notably, these were not associated with dysplastic changes.

In the present study, we observed areas of IM in 28 % of the ITAC specimens analyzed. This higher frequency in comparison with previous studies may depend on the selection methods that included the use of three immunohistochemical markers of intestinal differentiation and on the characteristics of our series of ITACs, which includes a high percentage of workers exposed to leather or wood dusts. However, the chances of detecting small foci of IM adjacent to ITAC are likely to be influenced by the sampling of the surgical material, and this may also explain the variable prevalence of sinonasal IM reported in the literature.

The hypothesis that these metaplastic foci may represent the precursor lesion of ITAC is reinforced by our observation that they are often associated with dysplastic changes of the metaplastic epithelium, including the presence of nuclear

enlargement, hyperchromasia, loss of nuclear polarity, and presence of prominent nucleoli. These morphologic changes are the key features of other precancerous conditions associated with IM, such as dysplasia in Barrett's esophagus and gastric dysplasia, and are considered a key step in Barrett's esophagus and gastric carcinogenesis [4, 7].

Our immunohistochemical study confirms that sinonasal IM is characterized by the expression of markers such as CK20, CDX2, and MUC2. CK20 and CDX2, in particular, were expressed in all the cases, and this is of particular interest because CDX2 has been implicated in the pathogenesis of IM in gastric and esophageal mucosa. In a CDX2-transgenic mouse model, CDX2 overexpression was associated with the appearance of foci of IM in gastric mucosa and CDX2 expression emerged before the expression of intestinal marker genes, indicating that this gene may lead the changes driving to IM [8]. Interestingly, in these models, the IM lesions frequently evolved into cancerous lesions, and this process was shortened when CDX2-transgenic mice were crossed with p53 deficient mice [8]. Accordingly, foci of IM from human gastric mucosa frequently harbor TP53 gene mutations [9–11], and TP53 mutation and inactivation by LOH at 17p, as well as CDX2 expression play an important role in the development of IM in Barrett's esophagus and its progression to esophageal adenocarcinoma [12, 13]. Here, we first report that sinonasal IM associated with ITAC frequently shows overexpression of p53 and may harbor the same TP53 gene mutation present in the adjacent ITAC. Similar observations have been made in carcinogenic sequence of Barrett's esophagus to esophageal adenocarcinoma [14], where the same TP53 mutation is frequently present in high-grade dysplasia and subsequent carcinoma, as well as in gastric tumorigenesis [15].

The frequency of TP53 mutations in ITAC has been reported to vary between 18 and 86 % [16–20], and loss of heterozygosity at the 17p13 locus that harbors the TP53 gene has been observed in 58 % of the cases [17]. Three of six ITACs analyzed in this study showed TP53 missense mutations and were all from patients with occupational exposure to wood or leather dusts. The most frequent TP53 alterations detected in ITAC have been G>A transitions, which are also strongly associated with an occupational history of wood or leather dust exposure [17, 19, 20].

Overexpression of cyclin D1, a key regulator of cell cycle, has been described in a wide variety of malignancies including head and neck squamous cell carcinomas, and it has been implicated in the early phases of carcinogenesis, in the progression from preneoplastic lesions to invasive carcinoma [21, 22]. The results of our immunohistochemical study do not allow a definitive conclusion regarding the involvement of cyclin D1 in the early phases of sinonasal ITAC development, because, although it was detected in areas of IM, this marker was expressed in inflamed sinonasal mucosa at comparable levels. Nevertheless, we observed that cyclin D1 is frequently over-expressed in ITACs, and this is in agreement with previous results showing that the CCND1 gene, which encodes for cyclin D1, is amplified in ethmoid sinus adenocarcinomas, although the histologic subtype was not further specified in this study [23]. Similarly, we did not observe any difference in terms of proliferative activity assessed as Ki67LI between the metaplastic foci and normal mucosa, while ITACs showed a significantly higher proliferation rate. However, it should be noted that the series of cases analyzed is small.

Previous study conducted on sinonasal mucosa biopsies obtained from subjects exposed to wood dust [24, 25] and to leather dust [26], mostly reported non-specific changes of the sinonasal mucosa, the most frequent being squamous metaplasia, cuboidal metaplasia, and goblet cell hyperplasia, while IM was not identified. This may be due to sampling problems, since a small biopsy of the sinonasal mucosa is quite unlike to include IM areas composed of groups of few cells. Alternatively, IM may be a late event that directly precedes the development of ITAC.

In conclusion, our data suggest the existence of a clonal relationship between areas of IM and the adjacent invasive adenocarcinoma. Indeed, in our series, 28 % of ITACs was associated with areas of IM, which frequently presented dysplastic changes (6 of 8, 75 %), and in two cases, there were identical types of TP53-gene mutations. This indicates that IM may represent a precursor of ITAC and suggests the existence of a field effect determined by exposure to carcinogens. A better understanding of the carcinogenic sequence leading to the development of sinonasal ITAC may allow a more precise identification of the patients at risk and may help to implement preventive strategies.

Acknowledgments This paper was supported in part by a grant from Istituto Toscano Tumori (ITT).

Conflict of interest The authors declare that they have no conflict of interest.

References

1. Choi HR, Sturgis EM, Rashid A, DeMonte F, Luna MA, Batsakis JG, El-Naggar AK (2003) Sinonasal adenocarcinoma: evidence for histogenetic divergence of the enteric and nonenteric phenotypes. Hum Pathol 34:1101–7
2. Kennedy MT, Jordan RC, Berean KW, Perez-Ordoñez B (2004) Expression pattern of CK7, CK20, CDX-2, and villin in intestinal-type sinonasal adenocarcinoma. J Clin Pathol 57:932–7
3. Vivanco B, Llorente JL, Perez-Escuredo J, Alvarez Marcos C, Fresno MF, Hermsen MA (2011) Benign lesions in mucosa adjacent to intestinal-type sinonasal adenocarcinoma. Patholog Res Int 2011: 230147
4. Lauwers GY (2003) Defining the pathologic diagnosis of metaplasia, atrophy, dysplasia, and gastric adenocarcinoma. J Clin Gastroenterol 36:S37–43

5. Franchi A, Massi D, Palomba A, Biancalani M, Santucci M (2004) CDX-2, cytokeratin 7 and cytokeratin 20 immunohistochemical expression in the differential diagnosis of primary adenocarcinomas of the sinonasal tract. Virchows Arch 445:63–7
6. Franchi A, Miligi L, Palomba A, Giovannetti L, Santucci M (2011) Sinonasal carcinomas: recent advances in molecular and phenotypic characterization and their clinical implications. Crit Rev Oncol Hematol 79:265–77
7. Sanders DSA, Taniere P, Harrison RF, Jankowski JAZ (2003) Clinical and molecular pathology of the metaplasia-dysplasia-carcinoma sequence in Barrett's oesophagus. Curr Diagn Pathol 9: 235–241
8. Mutoh H, Hakamata Y, Sato K, Eda A, Yanaka I, Honda S, Osawa H, Kaneko Y, Sugano K (2002) Conversion of gastric mucosa to intestinal metaplasia in Cdx2-expressing transgenic mice. Biochem Biophys Res Commun 294:470–9
9. Sugano K (2013) Premalignant conditions of gastric cancer. J Gastroenterol Hepatol 28:906–911
10. Karaman A, Kabalar ME, Binici DN, Oztürk C, Pirim I (2010) Genetic alterations in gastric precancerous lesions. Genet Couns 21:439–50
11. Morgan C, Jenkins GJ, Ashton T, Griffiths AP, Baxter JN, Parry EM, Parry JM (2003) Detection of p53 mutations in precancerous gastric tissue. Br J Cancer 89:1314–9
12. Beilstein M, Silberg D (2002) Cellular and molecular mechanisms responsible for progression of Barrett's metaplasia to esophageal carcinoma. Gastroenterol Clin North Am 31:461–79
13. Khor TS, Alfaro EE, Ooi EM, Li Y, Srivastava A, Fujita H, Park Y, Kumarasinghe MP, Lauwers GY (2012) Divergent expression of MUC5AC, MUC6, MUC2, CD10, and CDX-2 in dysplasia and intramucosal adenocarcinomas with intestinal and foveolar morphology: is this evidence of distinct gastric and intestinal pathways to carcinogenesis in Barrett esophagus. Am J Surg Pathol 36:331–42
14. Bian YS, Osterheld MC, Bosman FT, Benhattar J, Fontolliet C (2001) p53 gene mutation and protein accumulation during neoplastic progression in Barrett's esophagus. Mod Pathol 14:397–403
15. Shiao YH, Rugge M, Correa P, Lehmann HP, Scheer WD (1994) p53 alteration in gastric precancerous lesions. Am J Pathol 144:511–7
16. Wu TT, Barnes L, Bakker A, Swalsky PA, Finkelstein SD (1996) K-ras-2 and p53 genotyping of intestinal-type adenocarcinoma of the nasal cavity and paranasal sinuses. Mod Pathol 9:199–204
17. Perrone F, Oggionni M, Birindelli S, Suardi S, Tabano S, Romano R, Moiraghi ML, Bimbi G, Quattrone P, Cantu G, Pierotti MA, Licitra L, Pilotti S (2003) TP53, p14ARF, p16INK4a and H-ras gene molecular analysis in intestinal-type adenocarcinoma of the nasal cavity and paranasal sinuses. Int J Cancer 105:196–203
18. Licitra L, Suardi S, Bossi P, Locati LD, Mariani L, Quattrone P, Lo Vullo S, Oggionni M, Olmi P, Cantù G, Pierotti MA, Pilotti S (2004) Prediction of TP53 status for primary cisplatin, fluorouracil, and leucovorin chemotherapy in ethmoid sinus intestinal-type adenocarcinoma. J Clin Oncol 22:4901–6
19. Holmila R, Bornholdt J, Heikkilä P, Suitiala T, Févotte J, Cyr D, Hansen J, Snellman SM, Dictor M, Steiniche T, Schlünssen V, Schneider T, Pukkala E, Savolainen K, Wolff H, Wallin H, Luce D, Husgafvel-Pursiainen K (2010) Mutations in TP53 tumor suppressor gene in wood dust-related sinonasal cancer. Int J Cancer 127:578–88
20. Pérez-Escuredo J, Martínez JG, Vivanco B, Marcos CÁ, Suárez C, Llorente JL, Hermsen MA (2012) Wood dust-related mutational profile of TP53 in intestinal-type sinonasal adenocarcinoma. Hum Pathol 43:1894–901
21. Pignataro L, Capaccio P, Pruneri G, Carboni N, Buffa R, Neri A, Ottaviani A (1998) The predictive value of p53, MDM-2, cyclin D1 and Ki67 in the progression from low-grade dysplasia towards carcinoma of the larynx. J Laryngol Otol 112:455–9
22. Papadimitrakopoulou VA, Izzo J, Mao L, Keck J, Hamilton D, Shin DM, El-Naggar A, den Hollander P, Liu D, Hittelman WN, Hong WK (2001) Cyclin D1 and p16 alterations in advanced premalignant lesions of the upper aerodigestive tract: role in response to chemoprevention and cancer development. Clin Cancer Res 7:3127–34
23. Nazar G, González MV, García JM, Llorente JL, Rodrigo JP, Suárez C (2006) Amplification of CCND1, EMS1, PIK3CA, and ERBB oncogenes in ethmoid sinus adenocarcinomas. Otolaryngol Head Neck Surg 135:135–9
24. Bussi M, Gervasio CF, Riontino E, Valente G, Ferrari L, Pira E, Cortesina G (2002) Study of ethmoidal mucosa in a population at occupational high risk of sinonasal adenocarcinoma. Acta Otolaryngol 122:197–201
25. Valente G, Ferrari L, Kerim S, Gervasio CF, Ricci E, Migliaretti G, Pira E, Bussi M (2004) Evidence of p53 immunohistochemical overexpression in ethmoidal mucosa of woodworkers. Cancer Detect Prev 28:99–106
26. Palomba A, Iaia TE, Biancalani M, Conti S, Battista G, Papaleo B, Franchi A (2008) A morphologic and immunohistochemical study of nasal mucosa in leatherworkers. Am J Rhinol 22:356–60